

## Structural and elastic properties studies of yttrium lead borotellurite glass doped with neodymium oxide

M. R. S. Nasuha<sup>a</sup>, H. Azhan<sup>b,\*</sup>, W. A. W. Razali<sup>b</sup>, L. Hasnimulyati<sup>b</sup>,  
Y. Norihan<sup>b</sup>

<sup>a</sup>*Faculty of Applied Sciences, Universiti Teknologi MARA, 40450 Shah Alam, Selangor, Malaysia*

<sup>b</sup>*Faculty of Applied Sciences, Universiti Teknologi MARA Pahang, 26400 Jengka, Pahang, Malaysia*

The Nd<sup>3+</sup> doped yttrium lead borotellurite glasses with the chemical composition (49-x)H<sub>3</sub>BO<sub>3</sub>-35TeO<sub>2</sub>-15PbO-1.0Y<sub>2</sub>O<sub>3</sub>-xNd<sub>2</sub>O<sub>3</sub> (x = 0.0, 0.5, 1.0, 1.5, 2.0, and 2.5 mol%) were successfully synthesised by using melt-quenching technique. The amorphous nature of all the glass samples were confirmed through the XRD spectra and various structural parameter were determined. The ultrasonic velocities and elastic moduli were measured from the measured density and ultrasonic velocities. From the analysis, it indicates that the physical properties of these glasses depend upon the role of Nd<sub>2</sub>O<sub>3</sub> content inside the glass system and the compositional changes of the glass system.

(Received June 10, 2021; Accepted August 4, 2021)

*Keyword:* Lead Borotellurite glass, Neodymium, Elastic moduli, Structural properties

### 1. Introduction

Glasses are increasingly used as host material for solid state laser based on rare earth ions. Since the quantum of efficiency of emission transition depends on the structural modification of the host material, the selection of host material is important [1]. Among oxide glass formers, tellurite glass is one of the suitable host material due to their excellent properties such as non-hygroscopic in nature, high refractive index, low crystalline rate as well as good infrared transmitters for wavelength up to 5 μm [2–4]. Furthermore, tellurite glass is also good for hosting rare earth ions since it provides low phonon energy which minimizes non-radiative relaxation rates of rare earths excited-state levels [5,6]. However, tellurite oxide needs other glass former or modifier to form a tellurite glass because of pure tellurium dioxide does not readily form a glass under normal quenching rates [7]. The addition of borate oxide into tellurite oxide caused some enhancement in glass stability and glass quality with an improvement in transparency as well as decrease the hygroscopic nature [8]. Besides, this combination also may change the structure of the base glass which then lead to the changes in the physical properties of the glass system [9]. In addition, the incorporation of lead oxide improves the glass forming ability and prevents the crystallization of the glass [9]. Other than that, the combination of yttrium oxide gives excellent properties to glass such as good chemical and thermal stability [11].

In this paper, a series of Nd<sup>3+</sup> doped Yttrium lead borotellurite glass with different composition of Nd<sub>2</sub>O<sub>3</sub> was studied and characterized in terms of their structural and elastic properties. Density, molar volume, ultrasonic velocities, XRD, FTIR and EDX will be carried out in order to observe the influence of Nd<sub>2</sub>O<sub>3</sub> content in this glass. To the best of authors knowledge, the structural and elastic analysis of Nd<sup>3+</sup> doped yttrium lead borotellurite glasses has not been fully studied. Thus, this work will reveal the important information for the future potential application of this glass system.

---

\* Corresponding author: dazhan@uitm.edu.my

## 2. Experimental procedure

### 2.1. Sample synthesis

A series of Nd<sup>3+</sup> doped yttrium lead borotellurite glasses were prepared by melt-quenching technique. The raw material for glass samples were prepared using chemical compounds with high purity analytical grade chemical from Sigma Aldrich (Germany), Riedel-De Haen (Germany), (United Kingdom) and Acros Organic (Belgium) with 99.9% purity for Nd<sub>2</sub>O<sub>3</sub>, for Y<sub>2</sub>O<sub>3</sub> (99.99% purity), for PbO (99.0% purity), for H<sub>3</sub>BO<sub>3</sub> (99.8% purity) and for TeO<sub>2</sub> (99% purity). To attain a homogenous mixture, all the weighed chemical compounds (each batch composition of about 15 g) were mixed for 1 hour by using a milling machine. The mixture was then transferred into an alumina crucible and melted in an electric box furnace for 30 minutes at a temperature of 1000 °C. The melt was quickly quenched to 400 °C by pouring the molten into a preheated stainless-steel mould. Then, the annealing process was carried out for 5 hours at temperature 400 °C to enhance the mechanical strength and to remove internal stress in the glass. Next, the samples were allowed to cool down slowly to room temperature in the furnace. Finally, the glass samples were well polished before being used for any characterization.

### 2.2. Sample characterization

The glass's density ( $\rho$ ) was obtained using Archimedes principle with distilled water as the immersion liquid. The density of the glass was measured using the following equation

$$\rho = \frac{a}{a-b} \rho_x \quad (1)$$

where  $a$  and  $b$  is the weight of glass sample in air and in distilled water respectively.  $\rho_x$  is the density of distilled water (1g/cm<sup>3</sup>).

The consequent molar volume ( $V_m$ ) was measured from the measured density by using the formula

$$V_m = \frac{M}{\rho} \quad (2)$$

where  $M$  indicates the total molecular weight of the glass composition and  $\rho$  is the density of the glass.

Other characterization performed includes the XRD using the X'Pert PRO / PANalytical Diffractometer, FTIR using the Perkin-Elmer Spectrum 100 FT-IR Spectrometer system and the EDX using the Oxford Instrument Energy-Dispersive Spectrometer. The longitudinal and shear ultrasonic velocities were calculated by the ultrasonic measurement system UT Flaw Detector ECHOGRAPH 1095 at room temperature. Both of ultrasonic velocities ( $v$ ) were measured using the relation

$$v = \frac{2d}{\Delta t} \quad (3)$$

where  $d$  is the thickness of the sample and  $\Delta t$  is the transit time. The elastic moduli included longitudinal (L), shear (G), bulk (K) and Young's modulus (E) of the glass samples were obtained from the calculated density and ultrasonic velocities using the expression

$$L = \rho V_L^2 \quad (4)$$

$$G = \rho V_s^2 \quad (5)$$

$$K = L - \frac{4}{3}G \quad (6)$$

$$E = 2G(1 + \sigma) \quad (7)$$

where  $\rho$ ,  $V_L$  and  $V_s$  are the calculated density, longitudinal and shear ultrasonic velocity respectively. The Poisson's ratio ( $\sigma$ ), microhardness ( $H$ ), softening temperature ( $T_s$ ) and Debye temperature ( $\theta_D$ ) were calculated by using the following equation

$$\sigma = \frac{L-2G}{2(L-G)} \quad (8)$$

$$H = \frac{(1-2\sigma)E}{6(1+\rho)} \quad (9)$$

$$T_s = \left( \frac{V_s^2 M}{c^2 \rho} \right) \quad (10)$$

where  $M$  is the average molecular weight and  $c$  is a constant that equal to  $0.5074 \times 10^5$  cm/Ks.

$$\theta_D = \frac{h}{k} \left( \frac{9N}{4\pi V} \right)^{1/3} V_m \quad (11)$$

where  $h$ ,  $k$  and  $(N/V)$  are the Plank's constant, Boltzmann constant and the number of vibrating atoms per unit volume respectively.  $N/V$  is equal to  $(PN_A)$  where  $P$  is the number of atoms in the chemical formula and  $N_A$  is the Avogadro number. Meanwhile,  $V_m$  is the mean sound velocity that can be defined by the relation

$$V_m = \left[ \frac{(1/V_L^3) + (2/V_s^3)}{3} \right]^{-1/3} \quad (12)$$

### 3. Results and discussion

$\text{Nd}^{3+}$  doped yttrium lead borotellurite glasses are well prepared by using melt-quenching method. A glass series of  $(49-x)\text{H}_3\text{BO}_3\text{-}35\text{TeO}_2\text{-}15\text{PbO}\text{-}1.0\text{Y}_2\text{O}_3\text{-}x\text{Nd}_2\text{O}_3$  ( $x = 0.0, 0.5, 1.0, 1.5, 2.0, \text{ and } 2.5$  mol%) which the composition are presented in Table 1 below are well obtained. The glass samples are visualized in a good quality since they present no sign of vitrification. Besides that, the colour of the glass samples changes with respect to their composition as they vary from light purple to bright purple due to the existence of neodymium content. For undoped neodymium, the glass sample shows the colour of lime yellow which can be related to the existence of yttrium oxide inside the glass sample as reported by El-Mallawany (1998) [12]. The XRD patterns of  $\text{Nd}^{3+}$  doped yttrium lead borotellurite glasses are shown in Figure 1. This result clearly reveals that the absence of sharp peaks in the XRD pattern indicates that the glasses are amorphous.

Table 1. Composition of  $(49-x)\text{H}_3\text{BO}_3\text{-}35\text{TeO}_2\text{-}15\text{PbO}\text{-}1.0\text{Y}_2\text{O}_3\text{-}x\text{Nd}_2\text{O}_3$  glass system.

Nd <sub>2</sub> O <sub>3</sub> Concentration (mol%)	Nominal Composition (mol%)					Remark
	Nd <sub>2</sub> O <sub>3</sub>	H <sub>3</sub> BO <sub>3</sub>	TeO <sub>2</sub>	PbO	Y <sub>2</sub> O <sub>3</sub>	
0.0	0.0	49.0	35.0	15.0	1.0	Lime yellow
0.5	0.5	48.5	35.0	15.0	1.0	Light purple
1.0	1.0	48.0	35.0	15.0	1.0	Light purple
1.5	1.5	47.5	35.0	15.0	1.0	Bright purple
2.0	2.0	47.0	35.0	15.0	1.0	Bright purple
2.5	2.5	46.5	35.0	15.0	1.0	Bright purple

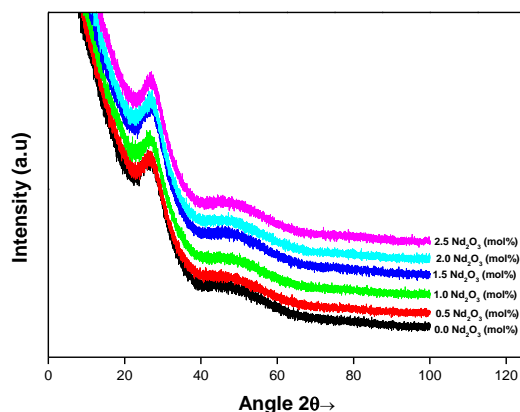


Fig. 1. XRD pattern of  $\text{Nd}^{3+}$  doped yttrium lead borotellurite glasses.

The effect of composition on structural changes in the glass system can be obtained by measuring the value of density and molar volume. The prepared glass densities increased from  $4.591 \text{ gcm}^{-3}$  to  $5.286 \text{ gcm}^{-3}$  as the  $\text{Nd}_2\text{O}_3$  content increased from 0 to 2.5 mol%. Meanwhile, the molar volume results are found to be inversely proportional to the results of density. The results decreased from  $26.551 \text{ cm}^3/\text{mol}$  to  $24.360 \text{ cm}^3/\text{mol}$  as the  $\text{Nd}_2\text{O}_3$  content increased. All the density and molar volume results are plotted with respect to  $\text{Nd}_2\text{O}_3$  content as shown in Figure 2.

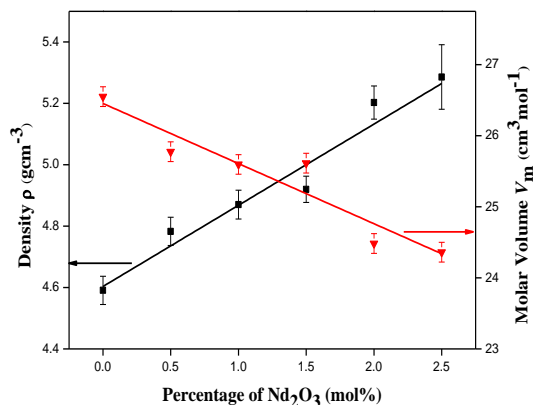


Fig. 2. Plot of Density and Molar Volume of Yttrium Lead Borotellurite Glasses with Respect to  $\text{Nd}_2\text{O}_3$  Content.

The increase in density may be connected to the replacement of lower molecular weight of  $\text{H}_3\text{BO}_3$  ( $61.83 \text{ g/mol}$ ) with a higher molecular weight of  $\text{Nd}_2\text{O}_3$  ( $336.48 \text{ g/mol}$ ) in the glass network which results in the increase of total molecular weight of the glass [13]. The molar volume of the prepared glasses decreases as the concentration of  $\text{Nd}^{3+}$  ions increase. The decreasing trend of the molar volume is possibly attributed to decrease in interatomic spacing or the decrease in the bond length between atoms of glass network, which leads to formation of a compact glass structure [14].

The FTIR spectra for the studied  $\text{Nd}^{3+}$  ions doped yttrium lead borotellurite glasses are presented in Figure 3. A deconvolution process using Origin 8.5 software was performed to identify the vibrational band (B) of each structural unit and also to measure the relative band area (A) under the absorption curve for each band which corresponds to the amount of each molecular component that exist in the glass system [15]. The deconvoluted FTIR spectra is presented in Figure 4 and the deconvolution parameter, IR band center and relative band area

for each peak of every glass sample against concentration of  $\text{Nd}_2\text{O}_3$  is listed in Table 2. The appearance of absorption bands in the range of  $649\text{--}661\text{ cm}^{-1}$  is assigned to the stretching vibration of Te-O bonds in trigonal bipyramidal, ( $\text{TeO}_4$ ) structural unit which illustrates the presence of bridging oxygen (BO) in the glass system. The bands in the range of  $693\text{--}700\text{ cm}^{-1}$  is attributed to the stretching vibrations of Te-O in ( $\text{TeO}_3$ ) trigonal pyramidal, groups. Then, the bands located around  $832\text{--}955\text{ cm}^{-1}$  and  $1063\text{--}1097\text{ cm}^{-1}$  are due to the stretching vibrations of B-O bonds of  $\text{BO}_4$  tetrahedral structural units. The band observed in the range  $1212\text{--}1219\text{ cm}^{-1}$  are attributed to the Te-O-Pb stretching vibrations. The last bands are noticed at  $1311\text{--}1360\text{ cm}^{-1}$  are ascribed to stretching vibration of the B-O bond in  $\text{BO}_3$  structural units.

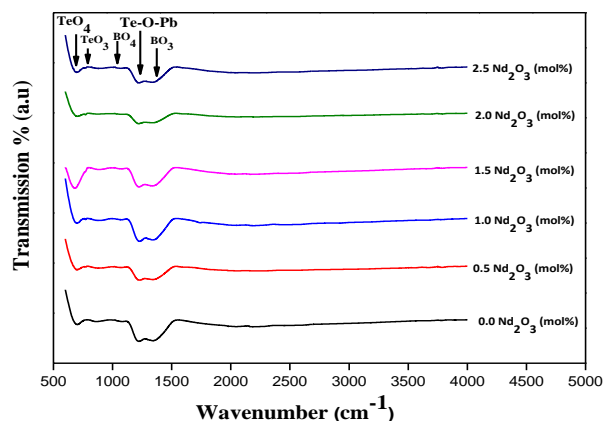


Fig. 3. FTIR Spectra of  $\text{Nd}^{3+}$  doped yttrium lead borotellurite glasses.

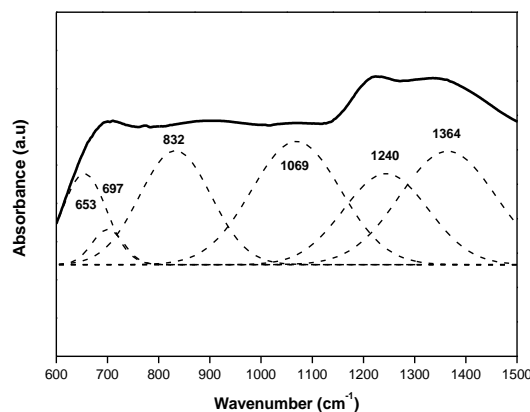


Fig. 4. Deconvolution of FTIR Spectra.

From Table 2, the relative band area of the structural units is varied as the concentration of  $\text{Nd}_2\text{O}_3$  increase from 0.0 mol% to 2.5 mol% which indicates that the structure of the glass change with the addition of dopant. The increase in relative band area of the  $\text{TeO}_4$  and  $\text{BO}_4$  structural units indicates that the closely packed network arises due to the formation of more bridging oxygens (BOs) [16], while the decrease indicates that the  $\text{TeO}_4$  and  $\text{BO}_4$  structural units are unstable and transformed into  $\text{TeO}_3$  and  $\text{BO}_3$  structural units and non-bridging oxygens (NBO) atoms formed [17]. These results proved the transformation of  $\text{TeO}_4$  into  $\text{TeO}_3$  and  $\text{BO}_4$  into  $\text{BO}_3$  and vice versa as reported earlier by A. A. Ali et al., (2017) [18].

Table 2. IR Spectra Band and Relative Band Area of Nd<sup>3+</sup> doped yttrium lead borotellurite glasses.

Nd <sub>2</sub> O <sub>3</sub> concentration (mol%)	IR Spectra Band, B (cm <sup>-1</sup> ) and Relative Area, A (%)						
	0.0	B	668	693	901	1094	1215
	A	4.05	18.85	24.37	30.00	3.42	29.31
0.5	B	652	694	863	1068	1219	1340
	A	9.16	13.19	33.08	10.84	7.45	21.87
1.0	B	653	697	832	1071	1219	1360
	A	14.05	6.45	28.36	24.81	17.45	36.69
1.5	B	649	700	952	1063	1212	1340
	A	11.85	14.62	34.92	12.91	3.12	22.58
2.0	B	658	696	924	1097	1212	1355
	A	12.64	10.88	24.64	14.18	4.66	33.32
2.5	B	661	694	955	1089	1215	1311
	A	13.05	9.96	15.97	12.38	3.77	32.03
Assignments		TeO <sub>4</sub> Stretching vibration [19]	TeO <sub>3</sub> stretching vibration [20]	BO <sub>4</sub> stretching vibration [21]		Te-O-Pb stretching vibration [22]	BO <sub>3</sub> stretching vibration [23]

The summary of composition elements of the Nd<sup>3+</sup> doped yttrium lead borotellurite glasses are tabulated in Table 3. All the elements such as lead oxide, borate oxide, tellurite oxide, neodymium oxide, and yttrium oxide taken initially are present in the final composition with their appropriate amount. From the results obtained, all the compositions are found to be close to the expected formulations composition. The presence of neodymium oxide in the glass system is confirmed with the increment of composition of neodymium from 0 up to 0.026, respectively. This is clear evidence that the neodymium oxide is successfully added into the glass structure of yttrium lead borotellurite glasses system.

Table 3. Summary of Composition Elements in Nd<sup>3+</sup> doped yttrium lead borotellurite glasses.

Nd <sub>2</sub> O <sub>3</sub> Concentration (mol%)	Stoichiometry	B	Te	Pb	Nd	Y
0.0	Initial	0.490	0.350	0.150	0.000	0.010
	From EDX	0.428	0.356	0.141	0.000	0.008
0.5	Initial	0.485	0.350	0.150	0.005	0.010
	From EDX	0.303	0.316	0.142	0.004	0.010
1.0	Initial	0.480	0.350	0.150	0.010	0.010
	From EDX	0.364	0.278	0.142	0.006	0.007
1.5	Initial	0.475	0.350	0.150	0.015	0.010
	From EDX	0.361	0.315	0.133	0.014	0.010
2.0	Initial	0.470	0.350	0.150	0.020	0.010
	From EDX	0.491	0.334	0.138	0.020	0.010
2.5	Initial	0.465	0.350	0.150	0.025	0.010
	From EDX	0.460	0.350	0.149	0.026	0.010

The results of longitudinal and shear velocity at room temperature for the yttrium lead borotellurite glasses as a function of Nd<sub>2</sub>O<sub>3</sub> content are tabulated in Table 4 and plotted in Figure 5. Both velocities increase as Nd<sub>2</sub>O<sub>3</sub> content increases. This increment trend indicates that the rigidity and strength of the glass network increases [24]. This is due to the addition of Nd<sub>2</sub>O<sub>3</sub> content in the glass network that breaking up bonds and fill the interstitial position within the vitreous network and causes the formation of more bridging oxygen. Besides that, the

increase in both ultrasonic velocities may also be due to the increasing packing density of the glass network [25].

Table 4. Longitudinal velocity  $V_L$ , Shear velocity  $V_s$  and Elastic moduli of  $Nd^{3+}$  doped yttrium lead borotellurite glasses.

$Nd_2O_3$ Concentration (mol%)	$V_L$ (m/s)	$V_s$ (m/s)	$L$ (GPa)	$G$ (GPa)	$K$ (GPa)	$E$ (GPa)
0.0	3840	2277	67.70	23.80	35.96	58.50
0.5	3798	2224	68.99	23.66	37.45	58.63
1.0	3902	2238	74.15	24.39	41.63	61.22
1.5	4000	2267	78.72	25.29	45.01	63.89
2.0	4042	2270	85.01	26.81	49.26	68.08
2.5	4145	2283	90.82	27.55	54.08	70.66

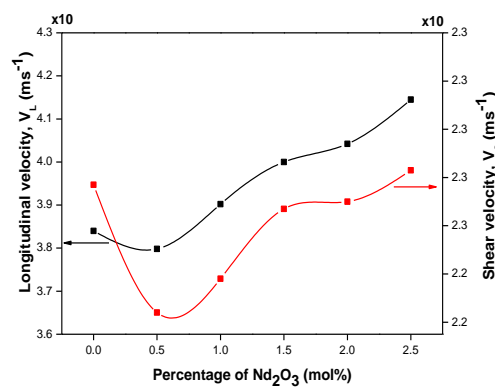


Fig. 5. Longitudinal and Shear Velocity of Yttrium Lead Borotellurite Glasses with Respect to  $Nd_2O_3$  Content.

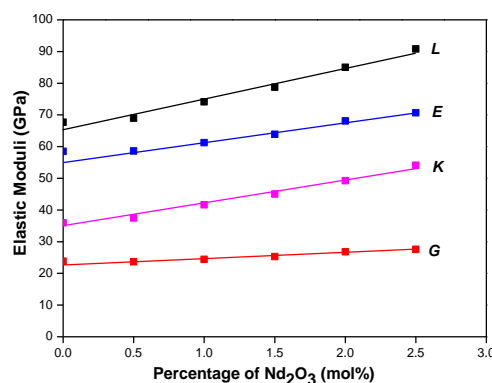


Fig. 6. The Elastic Moduli of Yttrium Lead Borotellurite Glasses with Respect to  $Nd_2O_3$  Content.

Figure 6 represents the plot of elastic moduli of yttrium lead borotellurite glasses versus the  $Nd_2O_3$  content. The trend of results is same to both of ultrasonic velocities. Based on Figure 6, the value of elastic moduli increases as the concentration of  $Nd_2O_3$  content increased. The increasing trend of elastic moduli indicates the increasing packing density of the glass due to the transformation from non-bridging oxygen to bridging oxygen atoms. In this study, the structural units of  $BO_3$  and  $TeO_3$  are transformed to  $BO_4$  and  $TeO_4$  respectively. The increase in elastic moduli can also be assigned to the increase of glass rigidity, resulting from an increase in the packing density of the glass network [26].

Table 5 shows the calculated results of Poisson's ratio, microhardness, softening temperature and Debye temperature. Rajendran et al. (2003) stated that, the Poisson's ratio will be affected by the changes in the cross-link density. Poisson's ratio of between 0.1 and 0.2 shows a high cross-link density in the glass structure while the Poisson's ratio between 0.3 to 0.5 presents, the structure has a low cross-link density [27].

Table 5. Poisson's ratio, Microhardness, Softening Temperature and Debye Temperature.

Nd <sub>2</sub> O <sub>3</sub> Concentration (mol%)	$\sigma$	H (GPa)	T <sub>s</sub> (K)	$\theta_D$ (K)
0.0	0.229	4.303	565.62	346.7
0.5	0.239	3.915	306.57	342.4
1.0	0.255	3.986	323.50	345.7
1.5	0.263	3.988	366.65	350.5
2.0	0.270	4.117	459.52	356.2
2.5	0.282	3.999	551.71	359.4

The results of Poisson's ratio observed in this glass network presents an increment trend from 0.229 to 0.282 with the addition of Nd<sub>2</sub>O<sub>3</sub> from 0 to 2.5 mol%. From these results, it is found that these studied glasses have high cross-link density. The increment trend in Poisson's ratio may be related to the the formation of non-bridging oxygen as more Nd<sub>2</sub>O<sub>3</sub> content introduced in the glass system which weakens the structure of the glass network [28]. The results of microhardness of the studied glass shows an initially increasing pattern from 3.915 GPa to 4.117 GPa before slightly decrease to 3.999 GPa as the concentration of Nd<sub>2</sub>O<sub>3</sub> increases from 0.5 mol% to 2.5 mol%. Such a pattern is probably related to the creation of bridging oxygen atoms from BO<sub>3</sub> to BO<sub>4</sub> and TeO<sub>3</sub> to TeO<sub>4</sub> structural units [29]. These structural changes cause an increase in rigidity and compactness of the glass system and can be the reason behind the increasing trend in microhardness [30]. Softening temperature is defined as the temperature at which viscous flow changes to plastic flow [31] and this parameter is used to determine the temperature stability of the glass. Whereas, Debye temperature can be describes as the properties arising from atomic vibration and is directly proportional to the mean ultrasonic velocity,  $V_m$  [32]. From the obtained results, the softening temperature and Debye temperature present a similar increment trend behaviour as the Nd<sub>2</sub>O<sub>3</sub> content increases. The optimum value of softening temperature at 2.5 mol% of Nd<sub>2</sub>O<sub>3</sub> indicates the higher stability of its elastic properties due to the increase in the number of atoms and ultrasonic velocities of the glass sample [33]. Meanwhile, the greater value of Debye temperature indicates the strengthening of the glass that can be related to the creation of bridging oxygen. These increasing trends of results indicates an increase in the rigidity of the glass system [34].

#### 4. Conclusion

The amorphous nature of these glasses is confirmed through the XRD pattern. The incorporation of Nd<sub>2</sub>O<sub>3</sub> in yttrium lead borotellurite glass showed that the glass system's density increases, and molar volume decreases with the increases of Nd<sub>2</sub>O<sub>3</sub> content. This is related to the replacement of the higher molecular weight of Nd<sub>2</sub>O<sub>3</sub> in the glass system. FTIR spectral study reveals the existance of Te-O bonds in TeO<sub>4</sub>, TeO<sub>3</sub>, and B-O bonds in BO<sub>4</sub> and BO<sub>3</sub> in the prepared glasses. From EDX analysis, all the elements of lead oxide, borate oxide, tellurite oxide, neodymium oxide and yttrium oxide are identified and confirmed that the glass samples are free from contamination. Longitudinal and shear ultrasonic velocities increases when the Nd<sub>2</sub>O<sub>3</sub> content is added from 0.5 mol% to 2.5 mol%.



These results are assigned to the increase in rigidity and strength of the glass network as well as elastic moduli. The values of Poisson's ratio are found to increase in the range 0.229 to 0.282 as the  $\text{Nd}_2\text{O}_3$  concentration increase from 0 to 2.5 mol%. This specifies that the glass samples possess a high cross-link density. The inclusion of  $\text{Nd}_2\text{O}_3$  content into the glass system gives an enhancement to softening temperature and Debye temperature which can be related to an increase in the number of atoms as well as the creation of bridging oxygen atoms.

### Acknowledgments

The author wishes to thank the Ministry of Higher Education (MOHE), Malaysia for the financial support to carry out this research through Fundamental Research Grant Scheme (FRGS) no. 600-IRMI/FRGS 5/3 (039/2019).

### References

- [1] Saba Farhan. H, Australian Journal of Basic and Applied Sciences, **11**(9), 171 (2017)
- [2] M. I. Sayyed, Journal of Alloys and Compounds, **688**, 111 (2016)
- [3] G. Lakshiminarayana, Kawa M. Kaky, S.O. Baki, Song Ye, A. Lira, I.V. Kityk, M.A. Mahdi, Journal of Alloys and Compounds, **686**, 769 (2016)
- [4] X. Feng, P. Horak, F. Poletti, "Tellurite glass fibers for mid-infrared nonlinear applications", Chapter 14, 2017
- [5] M. Halimah, S. Nazrin, F. Muhammad, Chalcogenide Letters, **16**(8), 365 (2019)
- [6] S.Nazrin, M. Halimah, F. Muhammad, A.A. Latif, A.S. Asyikin, Chalcogenide Letters, **18**(1), 11 (2021)
- [7] Hirdesh, A. Kaur, A. Khanna, F. González, American Institute of Physics, **1832**, 070022 (2017)
- [8] A. Chagraoui, A. Tairi, K. Ajebli, H. Bensaid, A. Moussaoui, Journal of Alloys and Compounds, **495**(1), 67 (2010)
- [9] S. M. Aziz, M. R. Sahar, S. K. Ghoshal, Journal of Alloys and Compounds, **735**, 1119 (2018)
- [10] Riyatun, L. Rahmasari, A. Marzuki, IOP Conference Series: Materials Science and Engineering, **107**, 012036 (2016)
- [11] U. Prasad, J. Prakash, A. M. Kannan, Sustainable Energy & Fuels **4**(3), 1496 (2020)
- [12] R. El-Mallawany, A. Abousehly, A. A. El-Rahamani, E. Yousef, Materials Chemistry and Physics, **52**(2), 161 (1998)
- [13] A. A. Abdulbaset, M. K. Halimah, M. N. Azlan, Solid State Phenomena. **268**, 28 (2017).
- [14] A. A. Ali, H. M. Shaaban, A. Abdallah, Journal of Materials Research and Technology, **7**(3), 240 (2018)
- [15] N. Kaur, A. Khanna, Journal of Non-Crystalline Solids, **404**, 116 (2014)
- [16] M. K. Halimah, A. A. Awshah, A. M. Hamza, K. T. Chan, S. A. Umar, S. H. Alazoumi, Journal of Material Science Material in Electronic, **31**, 3785 (2020)
- [17] Y. S. Rammah, A. A. Ali, A. M. Abdelghany, A. A. Ali, A. M. Abdelghany, Journal of Molecular Structure, **1175**, 504 (2019)
- [18] A. A. Ali, Y. S. Rammah, R. El-mallawany, D. Soury, Measurement, **105**, 72 (2017)
- [19] F. M. Fudzi, H. M. Kamari, F. D. Muhammad, A. A. Latif, Z. Ismail, Journal of Materials Science and Chemical Engineering, **06**(04), 18 (2018)
- [20] N. Elkhoshkhany, M. A. Khatab, M. A. Kabary, Ceramics International, **44**, 2789 (2016).
- [21] F. A. Moustafa, A. M. Fayad, F. M. Ezz-Eldin, Journal of Non-Crystalline Solids, **376**, 18 (2013)
- [22] A. Noranizah, K. Azman, H. Azhan, E. S. Nurbaisyatul, M. Abdullah, Advanced Materials Research, **1107**, 391 (2015)
- [23] N. Berwal, S. Dhankhar, P. Sharma, R.S. Kundu, R. Punia, N. Kishore, Journal of Molecular Structure, **1127**, 636 (2017)

- [24] I. Zaitizila, M. K. Halimah, F. D. Muhammad, M. S. Nurisya, *Journal of Non-Crystalline Solids*, **492**, 50 (2018)
- [25] N. Suebsing, N. Chutithanapanon, P. Juntarat, R. Laopaiboon, C. Bootjomchai, *Journal of Physics: Conference Series*, **1144**, 012129 (2018)
- [26] A. Alatawi, Abdulrhman M. Alsharari, Shams A. M. Issa, M. Rashad, A. A .A. Darwish, Yasser B. Saddeek, H. O. Tekin, *Ceramics International*, **46**, 3534 (2020)
- [27] V. Rajendran, N. Palanivelu, B. K. Chaudhuri, K. Goswami, *Journal of Non-Crystalline Solids*, **320**, 95 (2003)
- [28] R. A. Tafida, M. K. Halimah, F. D. Muhammad, K.T. Chan, M. Y. Onimisi, A. Usman, A. M. Hamzad; S. A. Umar, *Materials Chemistry and Physics*, **246**, 122801 (2020)
- [29] A. Mardhiah, S. N. E. Shafieza, K. Azman, H. Azhan, *Material Science Forum*, **846**, 177 (2016)
- [30] Nibedita Sasmal, M. Garai, B. Karmakar, *Journal of Asian Ceramic Societies*, **4**, 29 (2016).
- [31] S. A. Umar, M. K. Halimah, M. N. Azlan, L. U. Grema, G. G. Ibrahim, A. F. Ahmad, A. M. Hamza & M. M. Dihom, *Springer Nature Journal*, **291**, (2020)
- [32] C. Bootjomchai, *Radiation Physics and Chemistry*, **110**, 96 (2015)
- [33] M. A. Sidkey, A. Abd. El-Moneim, L. Abd El-Latif, *Materials Chemistry and Physics*, **61**, 103 (1999)
- [34] E. S. Yousef, M. M. Elokr, Y. M. Aboudeif, *Journal of Molecular Structure*, **1108**, 257 (2016)